The Influence of Thermal Radiation on MHD Tangent Hyperbolic Fluid Flow with Zero Normal Flux of Nanoparticles over an Exponential Stretching Sheet

[1*]T. Gangaiah, [2]N. Saidulu, and [3]A. Venkata Lakshmi

[1]Department of Mathematics
Government Degree College
Mancherial, Telangana, India
[1]tgangaiah79@gmail.com

[2,3]Department of Mathematics
University College of Science
Osmania University
Hyderabad, India
[2]nampellysaidulu28@gmail.com; [3]akavaramvlr@gmail.com

*Corresponding Author

Abstract

This article presents the two-dimensional MHD flow of tangent hyperbolic fluid with zero normal flux of nano-particles over an exponentially stretching sheet in presence of thermal radiation. The governing system of non-linear partial differential equations along with boundary conditions for this fluid flow is converted into a system of non-linear ordinary differential equations by using appropriate similarity transformations. The reduced system is numerically solved by Runge-Kutta fourth order method with shooting technique. The effects of emerging non-dimensional parameters on velocity, temperature and nanoparticle volume fraction profiles have been discussed and presented graphically. Furthermore, the impacts of these parameters on skin friction coefficient and local Nusselt number at the sheet are exhibited and discussed. Noticed that the thermal boundary layer thickness enhanced with the increase in Weissenberg number, power-law index and radiation parameter whereas the velocity profiles and the skin friction coefficient decreases with an increase in Weissenberg number and power-law index.

Keywords: Thermal radiation; tangent hyperbolic; zero normal flux; exponentially stretching; Weissenberg number

MSC 2010 No.: 80A20, 76A02, 76W05, 74A15

1.   Introduction

In recent years, the study of boundary layer flow over a stretching sheet has lot of importance due to its numerous applications in industrial manufacturing processes such as wire drawing, hot rolling, manufacturing of plastic and rubber surfaces and many others. In all these cases both stretching and simultaneous cooling or heating have a decisive influence on the quality of the final products. Probably Sakiadis (1961) was the first who studied the boundary layer flow over a continuous solid surface moving with constant velocity. Crane (1970) extended this concept to the steady two-dimensional viscous fluid flow over a linearly stretching sheet and obtained a similar solution for the problem. Wang (1990) discussed the unsteady laminar flow of viscous fluid and computed similarity solutions. Later Magyari et al. (1999) investigated the steady boundary layer flow on a continuous stretching surface with exponential temperature distribution. Plenty of literature has been produced by researchers on boundary layer flows over stretching sheet.

The study of the magnetohydrodynamic (MHD) flow of an electrically conducting fluid is of considerable interest in modern metallurgical and metal-working processes. The process of fusing of metals, power generation systems and cooling of nuclear reactor are good examples of such fields. In biomedical field, MHD flow has many practical applications such as magnetic field effects on wound healing and MRI (Magnetic Resonance Imaging) to diagnose disease and surgical procedures. Many investigations were made to examine the effects of MHD flow over a stretching sheet under different aspects. Shankar et al. (1997) studied the effects of mass transfer on the MHD flow past an impulsively started infinite vertical plate with variable temperature or constant heat flux. Recently, Anderson (2002), Ishak et al. (2010), Hayat et al. (2011) and Madhu et al. (2016) produced some important literature on MHD flow over a stretching sheet.

An extensive research has been conducted on boundary layer flow and heat transfer over an exponentially stretching sheet due to its wider applications in technology. For instance, in the case of annealing and tinning of copper wires and many others. Many kinds of literature are also available on boundary layer flow over a stretching surface where the velocity of the stretching surface is assumed to be linearly proportional to the distance from the fixed origin. However, Gupta et al. (1977) argued that realistically stretching of plastic sheet may not necessarily be linear. Magyari et al. (1999) investigated the mass and heat transfer in the boundary layers over an exponentially stretching surface with an exponential temperature distribution both analytically and numerically. In the recent past many researchers like Odat et al. (2006), Akram et al. (2009), Gangaiah et al. (2018) investigated various effects of heat and mass transfer over an exponentially stretching sheet.

The term nanofluid means a liquid suspension containing ultra-fine particles (diameter less than 50 nm). Experiments have shown that thermal conductivity can be appreciably improved by incorporating nanoparticles in the base fluid Metals (Al, Cu) such as oxides (Al_2O_3), carbides (SiC), nitrides (AlN, SiN) or nonmetals (graphite, carbon nanotubes) contain these nanoparticles. The term "nanofluid" was proposed by Choi, referring to dispersions of nanoparticles in the base fluids such as water, ethylene glycol, and propylene glycol. Choi (1995) showed that the addition of a small amount (less than 1 percent by volume) of nanoparticles to conventional heat transfer liquids increased the thermal conductivity of the fluid up to approximately two times. The thermal conductivity enhancement characteristic of nanofluid was observed by Masuda et al. (1993).

Buongiorno (2006) discussed the reasons behind the enhancement in heat transfer for nanofluid and he found that Brownian diffusion and thermophoresis are the main causes for enhancement in thermal boudary layer. Later, Nield et al. (2009) investigated the natural convective boundary layer flow of a nanofluid employing Buongiorno model. Angayarkanni et al. (2015) reviewed on thermal properties of nanofluieds. Recently, CS Reddy et al. (2017), Saidulu et al. (2018) and many other investigated the MHD flow of nanofluid over an exponentially stretching sheet using several methods.

Extensive research work has been conducted on non-Newtonian fluids to analyze the thermo-physical characteristics due to their numerous industrial and technological applications. The classical Navier-Stokes equations are inadequate to understand the distinctive properties of non-Newtonian fluids. Due to the diversity of non-Newtonian fluids, there is no unique model available to analyze the entire behaviour of non-Newtonian fluids. Among several non-Newtonian models, the tangent hyperbolic fluid model is one of the important fluid models. From laboratory experiments, it is found that this model predicts shear thinning phenomenon very precisely. Ketchup, whipped cream, blood, printer ink, paint and nail polish are some examples of tangent hyperbolic fluids. Pop et al. (2001) presented the hyperbolic tangent fluid model in his e-book *Convective heat transfer : Mathematical and Computational Modelling of Viscous Fluids and Porous media* and it is extensively used in different laboratory experiments. Akram et al. (2009) discussed the peristaltic flow of hyperbolic tangent fluid through an asymmetric channel. Numerical solutions of MHD boundary layer flow of tangent hyperbolic fluid over stretching sheet was deliberated by Akbar et al. (2013). Recently, Prabhakar et al. (2016) discussed the effects of inclained Lorentz forces on hyperbolic tangent nanofluid over a stretching sheet with passive flow of nanoparticles. Due to its wide range of applications, many researchers studied various effects on a tangent hyperbolic fluid in recent years.

The aim of the present work is to establish the influence of thermal radiation on magnetohydrodynamic flow of tangent hyperbolic fluid over an exponentially stretching surface with zero normal flux of nanoparticles. In order to achieve this aim, the present paper is organized as follows: The tangent hyperbolic fluid model is described in Section 2. The fluid flow model explained in Section 3 and how the governing non-linear partial differential equations transformed to a non-linear ordinary differential equation with suitable similarity transforms explained in Section 4, method of solution. Section 5 explains how we solved the resulting system of ODE with boundary conditions using Runge-Kutta method with shooting technique. We analysed both the numerical and graphical results in Section 6. The key findings of the present work manifested in Section 7.

2.   Tangent hyperbolic fluid model

The constitutive equations for tangent hyperbolic fluid (Pop et al. (2001), Akram et al. (2009)) is given by

$$\mathbf{S} = -P\mathbf{I} + \tau, \tag{1}$$

$$\tau = -\left[\, \mu_\infty + (\mu_0 + \mu_\infty)\, \tanh(\Gamma\bar{\dot{\gamma}})^n \,\right]\bar{\dot{\gamma}}. \tag{2}$$

In the above equations, τ is extra stress tensor, μ_0 is the zero shear rate viscosity, μ_∞ is the

infinite shear rate viscosity, Γ is the time-dependent material constant, n is the power law index and $\bar{\dot{\gamma}}$ defined as

$$\bar{\dot{\gamma}} = \sqrt{\frac{1}{2}\sum_i\sum_j \bar{\dot{\gamma}}_{ij}\bar{\dot{\gamma}}_{ji}} = \sqrt{\frac{1}{2}\Pi}, \tag{3}$$

where $\Pi = \frac{1}{2}trac\left[gradV + (gradV)^T\right]^2$, which is defined as second invariant strain tensor. Consider the equation (2) for the case when $\mu_\infty = 0$, because it is not possible to discuss the problem for the infinite shear rate viscosity and since we considering the tangent hyperbolic fluid that describes shear thinning effects so $\Gamma\bar{\dot{\gamma}} << 1$. Then, equation (2) becomes,

$$\begin{aligned}\tau &= -\mu_0\left[\ (\Gamma\bar{\dot{\gamma}})^n\ \right]\bar{\dot{\gamma}} \\ &= -\mu_0\left[\ (1 + \Gamma\bar{\dot{\gamma}} - 1)^n\ \right]\bar{\dot{\gamma}} \\ &= -\mu_0\left[\ 1 + n\left(\Gamma\bar{\dot{\gamma}} - 1\right)\ \right]\bar{\dot{\gamma}}.\end{aligned} \tag{4}$$

3. Mathematical Formulation

Consider the steady, laminar, two-dimensional boundary layer incompressible flow of an electrically conducting tangent hyperbolic fluid with zero normal flux of nanoparticles over an exponentially stretching sheet coinciding with the plane $y = 0$ and the flow is confined to $y > 0$. The x-axis is taken along the stretching surface in the direction of the motion while the y-axis is perpendicular to it. Keeping the origin fixed, the sheet is then stretched with a velocity (U_w) varying linearly with the distance from the slit and T_w as the temperature at the surface. To neglect the gravitational effects, the mass flux of the nanoparticle at the wall is assumed to be zero. A variable magnetic field $B = B_0 e^{\frac{x}{2L}}$ is applied to the sheet, where B_0 is the initial strength of the magnetic field. Under these considerations, the governing equations of continuity, momentum, energy and concentration (Akbar et al. (2013), Prabhakar et al. (2016)) are written as follows:

$$\frac{\partial u}{\partial x} + \frac{\partial v}{\partial y} = 0, \tag{5}$$

$$u\frac{\partial u}{\partial x} + v\frac{\partial u}{\partial y} = \nu(1-n)\frac{\partial^2 u}{\partial y^2} + \sqrt{2}n\nu\Gamma\left(\frac{\partial u}{\partial y}\right)\left(\frac{\partial^2 u}{\partial y^2}\right) - \frac{\sigma B^2 u}{\rho}, \tag{6}$$

$$u\frac{\partial T}{\partial x} + v\frac{\partial T}{\partial y} = \alpha\frac{\partial^2 T}{\partial y^2} + \frac{1}{\rho c_p}\frac{\partial q_r}{\partial y} + \tau\left[D_B\frac{\partial C}{\partial y}\frac{\partial T}{\partial y} + \frac{D_T}{T_\infty}\left(\frac{\partial T}{\partial y}\right)^2\right], \tag{7}$$

$$u\frac{\partial C}{\partial x} + v\frac{\partial C}{\partial y} = D_B\frac{\partial^2 C}{\partial y^2} + \frac{D_T}{T_\infty}\frac{\partial^2 T}{\partial y^2}. \tag{8}$$

The boundary conditions associated with the problem are

$$\begin{aligned}u &= U_w,\ \ v = V_w,\ \ T = T_w,\ \ D_B\frac{\partial C}{\partial y} + \frac{D_T}{T_\infty}\frac{\partial T}{\partial y} = 0\ \text{ at }\ y = 0, \\ u &\to 0,\ \ T \to T_\infty,\ \ C \to C_\infty\ \text{ as }\ y \to \infty.\end{aligned} \tag{9}$$

In the above equations, u and v are velocity components in the x and y directions respectively, T is the fluid temperature, C is the concentration of the fluid, $\nu = \frac{\mu}{\rho}$ is the kinematic viscosity, μ is the coefficient of the viscosity, ρ is the fluid density, n is the power-law index, Γ is the time-dependent material constant, σ is the electrical conductivity, $B = B_0 e^{\frac{x}{2L}}$ is the variable magnetic field, $\alpha = \frac{k}{\rho c_p}$ is the thermal diffusivity of the fluid (where k is thermal conductivity and c_p is the

specific heat at constant pressure), q_r is the radiative heat flux, $\tau = \frac{(\rho c)_p}{(\rho c)_f}$ is the ratio of heat capacities of nanofluid $(\rho c)_p$ and base fluid $(\rho c)_f$ and D_B, D_T are Brownian, thermophoretic diffusion coefficients, respectively.

Also, $U_w = U_0 e^{\frac{x}{L}}$ is the stretching velocity, U_0 is the reference velocity, L is the characteristic length. $V_w > 0$ is the velocity of suction and $V_w < 0$ is the velocity of blowing and $V_w = -v_0 e^{\frac{x}{2L}}$ is a special type of velocity on the wall, where v_0 is the initial strength of the suction, $T_w = T_\infty + T_0 e^{\frac{x}{2L}}$ is the variable temperature at sheet with T_0 being a constant which measures the rate of temperature increase along the sheet T_∞ is the ambient fluid temperature and C_∞ is the ambient fluid concentration.

According to Roseland's approximation for radiation (Brewster (1992)), the radiative heat flux q_r is simplified as

$$q_r = -\frac{4\sigma^*}{3k^*} \frac{\partial T^4}{\partial y}, \tag{10}$$

where σ^* is the Stefan-Boltzmann constant and k^* is the absorption coefficient. Assume that the temperature differences, such as the term T^4 within the flow, may be expressed as a linear function of temperature. After neglecting higher-order terms, Taylor series expansion for T^4 about T_∞ we have

$$T^4 \cong 4T_\infty{}^3 T - 3T_\infty{}^4. \tag{11}$$

By using (10) and (11), we get

$$q_r = -\frac{16\sigma^* T_\infty{}^3}{3k^*} \frac{\partial T}{\partial y}. \tag{12}$$

4. Method of Solution

To illustrate the problem, we introduced the following similarity transformations to derive a system of ordinary differential equations from the given system of non-linear partial differential equations:

$$\psi(x,y) = \sqrt{2U_0 \nu L} \; e^{\frac{x}{2L}} f(\eta), \quad \eta(x,y) = \sqrt{\frac{U_0}{2\nu L}} \; e^{\frac{x}{2L}} y,$$

$$\theta(\eta) = \frac{T - T_\infty}{T_0} e^{\frac{-x}{2L}}, \quad \phi(\eta) = \frac{C - C_\infty}{C_0},$$

where η is the similarity variable, $f(\eta), \theta(\eta)$ and $\phi(\eta)$ are dimensionless stream, temperature and concentration functions respectively. Here, the continuity equation is satisfied by choosing a stream function $\psi(x,y)$ such that

$$u = \frac{\partial \psi}{\partial y}, \quad v = -\frac{\partial \psi}{\partial x},$$

and hence,

$$u = U_0 \, e^{\frac{x}{L}} \, f', \quad v = -\sqrt{\frac{U_0 \nu}{2L}} \; e^{\frac{x}{2L}} (\eta \, f' + f).$$

By substituting above transformations, (6) - (8) can be transformed into a system of ordinary differential equations such as,

$$\left[(1-n) + n\,We\,f''\right]f''' + ff'' - 2\left(f'\right)^2 - M\,f' = 0, \tag{13}$$

$$\frac{1}{Pr}\left(1 + \frac{4R}{3}\right)\theta'' + \theta'f - f'\theta + Nb(\theta'\phi') + Nt\left(\theta'\right)^2 = 0, \tag{14}$$

$$\phi'' + Pr\,Le\,\phi'\,f + \frac{Nt}{Nb}\,\theta'' = 0. \tag{15}$$

The corresponding dimensionless boundary conditions take the form

$$\begin{aligned} &f(\eta) = S, \quad f'(\eta) = 1, \quad \theta(\eta) = 1, \quad \phi'(\eta) = -\tfrac{Nt}{Nb}\theta'(\eta) \ \text{ at }\ \eta = 0\ \text{ and} \\ &f'(\eta) \to 0, \quad \theta(\eta) \to 0, \quad \phi(\eta) \to 0 \quad \text{as}\ \eta \to \infty. \end{aligned} \tag{16}$$

Here, the primes denote differentiation with respect to η, $We = \frac{\Gamma U_0^{\frac{3}{2}} e^{\frac{3x}{2l}}}{\nu L}$ is the Weissenberg number, $M = \frac{2L\sigma B_0^2}{U_0\rho}$ is the magnetic field parameter, $Pr = \frac{\mu c_p}{k} = \frac{\nu}{\alpha}$ is the Prandtl number, $R = \frac{4\sigma^* T_\infty^3}{kk^*}$ is the radiation parameter, $Nt = \frac{\tau D_T(T_w - T_\infty)}{T_\infty \nu}$ is the thermophoresis parameter, $Nb = \frac{\tau\,D_B\,C_w}{\nu}$ is the Brownian motion parameter, $Le = \frac{\alpha}{D_B}$ is the Lewis number and $S = v_0\sqrt{\frac{2L}{\nu U_0}} > 0$ (or $S < 0$) is the suction (or blowing) parameter.

The important physical quantities of this problem are the skin friction coefficient C_{f_x} and the local Nusselt number Nu_x which represents wall shear stress and the heat transfer rate respectively and they are defined as

$$C_{f_x} = \frac{\tau_w}{\rho\,U_w{}^2}, \quad Nu_x = \frac{x\,q_w}{k(T_w - T_\infty)}. \tag{17}$$

Here, τ_w, q_w represent wall shear stress, heat transfer rate at the surface of sheet respectively, and these quantities are defined as

$$\begin{aligned} &\tau_w = \mu\left[(1-n)(\tfrac{\partial u}{\partial y}) + \tfrac{n\,\Gamma}{\sqrt{2}}(\tfrac{\partial u}{\partial y})^2\right]_{y=y_0}, \\ &q_w = -k(\tfrac{\partial T}{\partial y})_{y=y_0}. \end{aligned} \tag{18}$$

After using similarity variables, the skin friction coefficient and local Nusselt number transformed to

$$(Re_x)^{\frac{1}{2}}C_{f_x} = \sqrt{\frac{x}{2L}}\left[(1-n)f''(0) + \frac{n}{2}\,We\,(f''(0))^2\right], \tag{19}$$

$$(Re_x)^{\frac{-1}{2}}Nu_x = \sqrt{\frac{x}{2L}}\left[-\theta'(0)\right]. \tag{20}$$

Here, $Re_x = \frac{x\,U_w}{\nu}$ is a local Reynolds number.

5. Numerical Method

The above equations (13) - (15) along with the boundary conditions (16) are highly nonlinear ordinary differential equations. In order to solve these equations numerically, we used Runge-Kutta fourth order method along with shooting technique which is described in Dulal (2010). Here it is important to choose the appropriate finite values of $\eta \to \infty$. In order to determine η_∞, we start with some initial guess value for some particular set of physical parameters to obtain $f''(0)$ and

$\theta'(0)$. Now use the following set of variables to reduce above set of differential equations (13) - (15) along with the boundary conditions (16) into a system of first-order differential equations.

$$
\begin{aligned}
f &= f_1, & f' &= f_2, & f'' &= f_3, \\
\theta &= f_4, & \theta' &= f_5, & \phi &= f_6, & \phi' &= f_7.
\end{aligned}
\tag{21}
$$

With these variables, we get the system of first-order differential equations as

$$
f_1' = f' = f_2,
\tag{22}
$$

$$
f_2' = f'' = f_3,
\tag{23}
$$

$$
f_3' = f''' = \frac{[\, 2(f_2)^2 - f_1\, f_3 + M\, f_2\,]}{[\,(1-n) + n\, We\, f_3\,]},
\tag{24}
$$

$$
f_4' = \theta' = f_5,
\tag{25}
$$

$$
f_5' = \theta'' = \frac{-Pr}{(1 + \frac{4R}{3})}\, [\, f_1\, f_5 - f_2\, f_4 + Nb\, f_5\, f_7 + Nt(f_5)^2\,],
\tag{26}
$$

$$
f_6' = \phi' = f_7,
\tag{27}
$$

$$
f_7' = \phi'' = -[\, Pr\, Le\, f_1\, f_7 + \frac{Nt}{Nb}\, f_5'\,].
\tag{28}
$$

The boundary conditions are modified as

$$
\begin{aligned}
f_1 &= S, & f_2 &= 1, & f_4 &= 1, & f_7 &= \tfrac{-Nt}{Nb}\, f_5 & \text{at } \eta = 0 \quad \text{and} \\
f_2 &\to 0, & f_4 &\to 0, & f_6 &\to 0 & & \text{as } \eta \to \infty.
\end{aligned}
\tag{29}
$$

In order to solve the system of equations (13) - (15) along with boundary conditions (16), we requires a value for $f''(0)$, $\theta'(0)$ and $\phi'(0)$. But no such value is given at the boundary. We chosen suitable guess functions for $f(\eta)$, $\theta(\eta)$ and $\phi(\eta)$ to calculate the values of $f''(0)$, $\theta'(0)$ and $\phi'(0)$ in MATLAB algorithm for Runge-Kutta method with shooting technique with step size $\Delta\eta = 0.01$. We compared the calculated values of $-\theta'(0)$ with existing results. The above procedure is repeated until we get the converged results within a tolerance limit of 10^{-5}.

6. Results and Discussion

In order to study, the behaviour of velocity, temperature and nanoparticle volume fraction profiles along with physical quantities skin friction coefficient (C_{f_x}) and local Nusselt number (Nu_x) for various values of the governing parameters namely, the magnetic field parameter (M), the suction parameter (S), the Prandtl number (Pr), the Lewis number (Le), Brownian motion parameter (Nb), thermophoresis parameter (Nt), the Weissenberg number (We), the radiation parameter (R) and the power-law index (n), we used the Runge-Kutta fourth order method with shooting technique and computed the numerical computations using MATLAB program and the results are reported in terms of Table 1 and graphs as shown in Figures 1-20. For numerical results and plotting graphs, we used $M = S = R = n = 0.1, Pr = 2.5, Le = 1, Nt = Nb = 0.5$ and $We = 0.3$. These values are treated common throughout the study except the varied values in respective figures and tables. To establish the numerical accuracy, for various values of Pr and the values of $[-\theta'(0)]$ are compared with the existing results in Table 1 in absence of nanofluid, magnetic field, viscous dissipation and suction and those are found in excellent agreement.

Table 1. Comparison of $[-\theta'(0)]$ for several values of Prandtl number Pr and radiation parameter R in absence of nanofluid with $M = S = We = n = 0$ and $Le = 1$

Pr	R	Bidin et al. (2009)	Ishak et al. (2010)	Swathi (2013)	Present results
1	0	0.9547	0.9548	0.9547	0.9548
2	0	1.4714	1.4715	1.4714	1.4715
3	0	1.8691	1.8691	1.8691	1.8691
1	0.5	0.6765			0.6775
2	0.5	1.0735		1.0735	1.0735
3	0.5	1.3807		1.3807	1.3807
1	1	0.5315	0.5312	0.5311	0.5353
2	2	0.8627		0.8626	0.8629
3	3	1.1214		1.1214	1.1214

Here, we discussed the graphical outcomes of the problem in a physical sense. The influence of magnetic field parameter M on the dimensionless velocity and temperature are shown in Figures 1 - 2, respectively. It is clear from the Figure1 that an increase in the magnetic field parameter reduces the velocity boundary layer. The magnetic field opposes the transport process. Actually, due to the increase in M leads to the increase of the Lorentz force and it produces much more resistance to the transport phenomena. It is also observed that from Figure 2, the temperature profiles increase with an increase in M. The Lorentz force has the tendency to increase the temperature in nanofluid motion. Consequently, the thermal boundary layer thickness become thicker for a stronger magnetic field. Figures 3 and 4 depict the influence of the suction parameter S on velocity and temperature profiles. It is evident from the figures that an increase in suction parameter decrease the velocity and temperature boundary layers. Due to the suction, the fluid is brought closer to the sheet and it thins velocity boundary layer thickness as well as thermal boundary layers thickness.
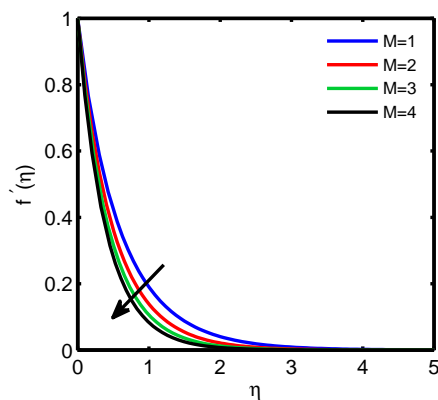
Figure 1. Velocity profiles for various values of M
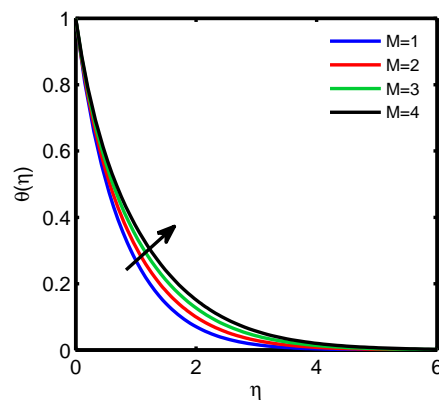
Figure 2. Temperature profiles for various values of M

Figures 5 and 6 illustrates the influence of Weissenberg number We on velocity and thermal boundary layers, respectively. Weissenberg number compares the viscous forces to the elastic forces. It is usually given by the relation of stress relaxation time of the fluid and a specific process time.

The increment in We increases the stress relaxation time of the fluid which increases the resistance of the flow and hence decreases the velocity boundary layer. Due to that viscoelastic forces as We increases the temperature boundary layer thickness increases. The effect of the power-law index n on the dimensionless velocity and temperature profiles are shown in Figures 7 and 8, respectively. It is observed that the increase in power-law index reduces the velocity profile since as n increases the fluid nature changes from shear thinning to shear thickening. It is seen from Figure 8 that the temperature increases with the increase of n.
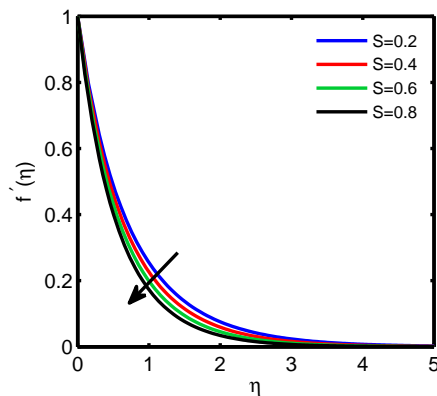
Figure 3. Velocity profiles for various values of S
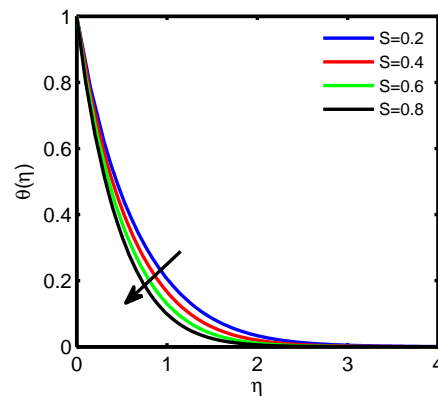
Figure 4. Temperature profiles for various values of S
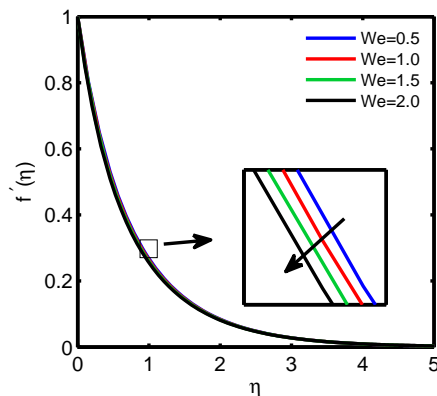
Figure 5. Velocity profiles for various values of We
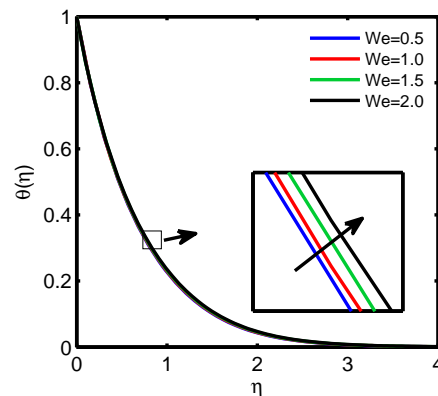
Figure 6. Temperature profiles for various values of We

The effect of the Prandtl number Pr on the temperature and nanoparticle volume fraction are depicted in Figures 9 and 10, respectively. The increase in Pr decreases the thermal diffusivity and hence reduces the thermal boundary layer thickness. The concentration boundary layer exhibits overshoot near the sheet for higher values of Pr, though the concentration boundary layer thickness reduces. Figure 11 explains the effect of radiation parameter R on thermal boundary layer. from graph, it is observed that the increase in R increases the temperature boundary layers. This result is expected because the presence of thermal radiation works as a heat source and so the quantity of heat added to the flow. The effect of Lewis number Le on the dimensionless nanoparticle volume fraction is plotted in Figure 12. It reveals that the concentration boundary layer thickness increases initially and later decreases as Le value increases.
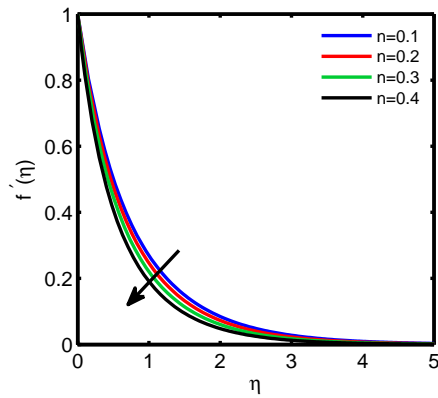
Figure 7. Velocity profiles for various values of n
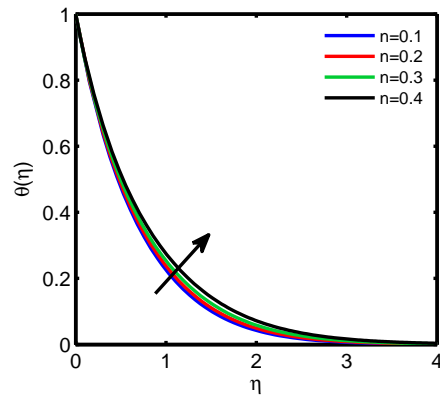
Figure 8. Temperature profiles for various values of n
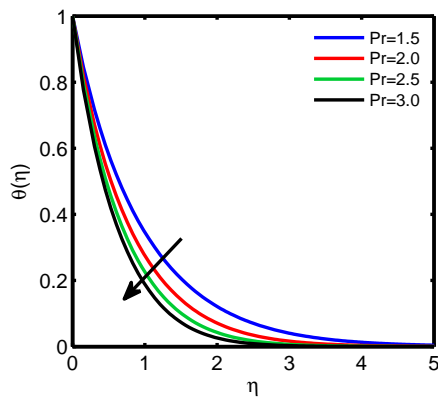
Figure 9. Temperature profiles for various values of Pr
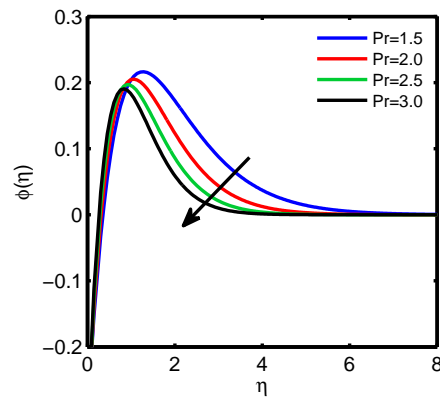
Figure 10. Nanoparticle volume fraction profiles for various values of Pr
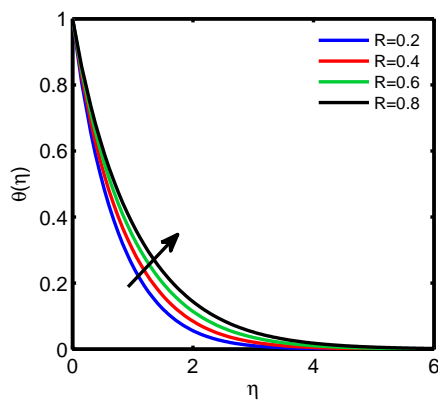
Figure 11. Temperature profiles for various values of R
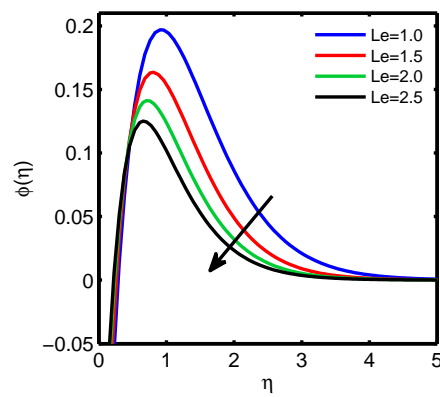
Figure 12. Nanoparticle volume fraction profiles for various values of Le

The impact of thermophoresis parameter Nt on temperature and concentration profiles is depicted in Figures 13 and 14, respectively. With an increase of Nt, it increases thermophoretic force which tends to move nanoparticles from hot to cold areas and hence, it increases the magnitude of temperature profiles. With an increment in Nt, the concentration boundary layer thickness increases and the overshoot near the wall is found. The effect of Brownian motion parameter Nb on the temperature and concentration are plotted in Figures 15 and 16, respectively. Due to the presence of nanoparticles in base fluid Brownian motion takes place and their collision with the fast-moving molecules in the fluid. Consequently the heat transfer characteristic of the fluid increases. Also, when the value of Nb increases, diffusion takes place and hence the concentration boundary layer thickness decreases.
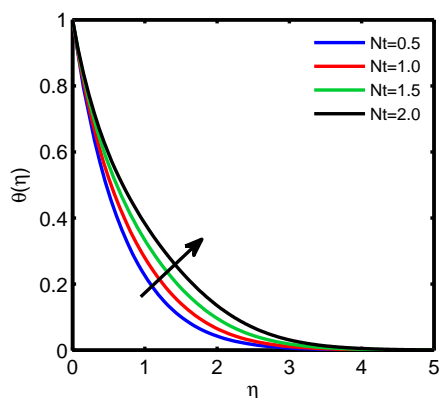
Figure 13. Temperature profiles for various values of Nt
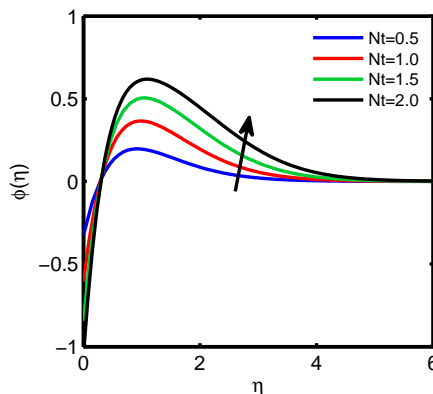
Figure 14. Nanoparticle volume fraction profiles for various values of Nt
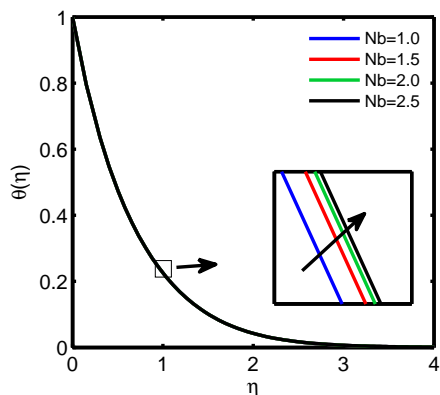
Figure 15. Temperature profiles for various values of Nb
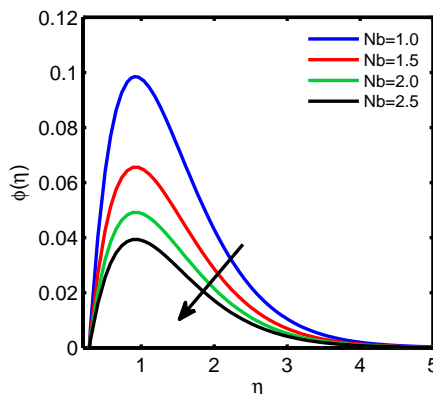
Figure 16. Nanoparticle volume fraction profiles for various values of Nb

Now, we discuss the variations of the physical quantities of engineering importance, that is, the skin friction coefficient $[C_{f_x}]$ and the local Nusselt number $[Nu_x]$ for various values of S, M, R, We and n. Here the quantities $f''(0)$ and $-\theta'(0)$ are related to the skin friction coefficient and the local Nusselt number, respectively. Figure 17 represents the behaviour of the skin friction coefficient $[f''(0)]$ with suction parameter S for three different values of Weissenberg number ($We = 0.5, 1, 1.5$). It is

found that skin friction coefficient decreases with an increase in S as well as an increase in We. Figure 18 displays the variation in skin friction coefficient $[f''(0)]$ with magnetic field parameter M for three different values of power-law index $(n = 0.1, 0.2, 0.3)$. from that graph, skin friction coefficient increases with an increase in M and n. Figures 19 and 20 explains the change in local Nusselt number $[-\theta'(0)]$ with radiation parameter R for three different values of power-law index $(n = 0.1, 0.2, 0.3)$ and Weissenberg number $(We = 0.5, 1, 1.5)$, respectively. From that, we conclude that local Nusselt number decrease as an increase in R and n as well as We.
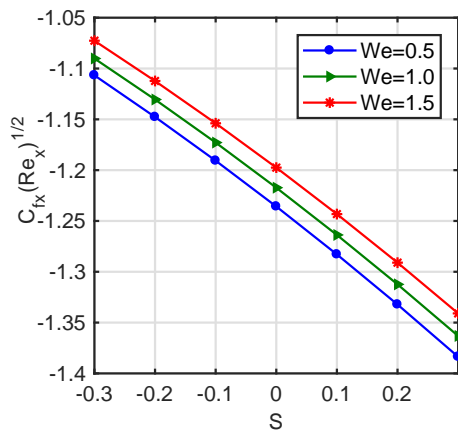
Figure 17. Variation in skin friction coefficient $[f''(0)]$ for various values of S and We
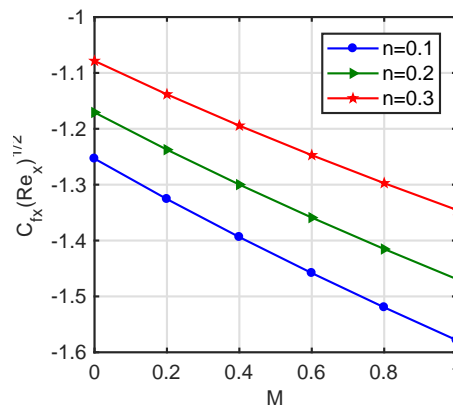
Figure 18. Variation in skin friction coefficient $[f''(0)]$ for various values of M and n
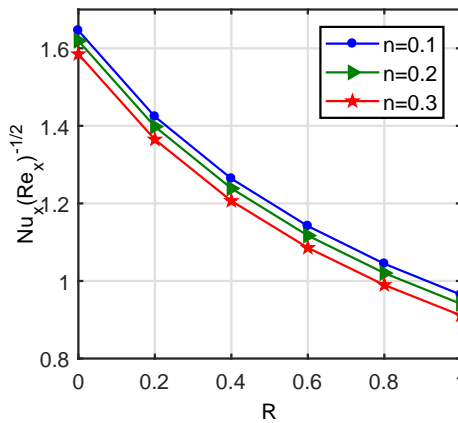
Figure 19. Variation in local Nusselt Number $[-\theta'(0)]$ for various values of R and n
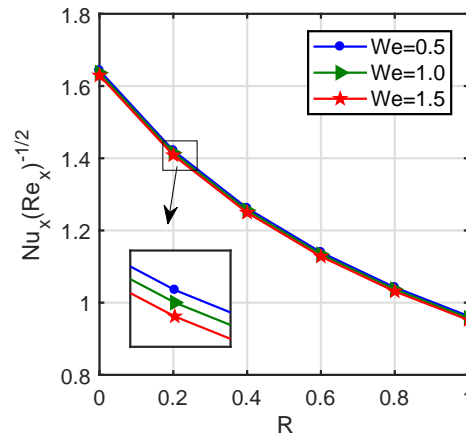
Figure 20. Variation in local Nusselt Number $[-\theta'(0)]$ for various values of R and We

7. Conclusions

In this paper, we numerically investigated the influence of thermal radiation and inclined magnetic force on hyperbolic tangent nanofluid with zero normal flux over an exponentially stretching sheet. In addition, heat source/sink parameter and thermal radiation parameters have been considered for the flow to analyze velocity, temperature and nanoparticle volume fraction profiles as well as the

skin friction coefficient and Nusselt number. The important findings of the present study are as follows:

- The velocity of the fluid, skin friction coefficient and Nusselt number reduced with increasing values of Weissenberg number while it increases the temperature.
- Increase in the magnetic field generates strong Lorentz force and hence it decreases the velocity of the fluid and increases the temperature profiles.
- Due to the suction, the fluid is brought closer to the sheet and it thins velocity boundary layer thickness as well as thermal boundary layers thickness.
- The temperature of the fluid enhanced with the radiation parameter, Lewis number, power-law index, thermophoresis parameter and Brownian parameter whereas decreases with Prandtl number.
- The concentration boundary layer thickness decreases with Brownian motion parameter, Prandtl number and Lewis number and increases with thermophoresis parameter.
- The skin friction coefficient $[f''(0)]$ decreases with an increase in magnetic field parameter, Weissenberg number, power law index and suction parameter.
- The local Nusselt number $[-\theta'(0)]$ increases with an increase Weissenberg number, magnetic field parameter and power-law index.

Acknowledgments

REFERENCES

Akbar, N.S., Nadeem, S., Haq, R.U. and Khan, Z.H. (2013). Numerical Solutions of Magnetohydrodynamic Boundary Layer Flow of Tangent Hyperbolic Fluid towards a Stretching Sheet, Indian Journal of Physics, Vol. 87, pp. 1121–1124.

Andersson, H. I. (2002). Slip Flow past a Stretching Surface, Acta Mechanica, Vol. 158, No. 1, pp. 121–125.

Angayarkanni and Philip, J. (2015), Review on Thermal Properties of nanofluids: Recent Developments, Advances in Colloid and Interface Science, Vol. 225, pp. 146–176.

Anuar, I. (2011). MHD Boundary Layer Flow due to an Exponentially Stretching Sheet with Radiation Effect, Sains Malaysiana, Vol. 40, No. 4, pp. 391–395.

Bidin, B. and Nazar, R. (2009). Numerical Solution of the Boundary Layer Flow over an Exponentially Stretching sheet with Thermal Radiation, European Journal of Scientific Research, Vol. 33, No. 4, pp. 710–717.

Brewster, M. Q. (1992). *Thermal Radiative Transfer and Properties*, John Wiley and Sons, New York, USA.

Buongiorno, J. (2006). Convective Transport in Nanofluids, Journal of Heat Transfer, Vol. 128, No. 3, pp. 240–250.

Carragher, P. and Crane, L.J. (1982). Heat Transfer on a Continuous Stretching Sheet, Zeitschrift fr Angewandte Mathematik and Mechanik, Vol. 62, No. 10, pp. 564–565.

Choi, S.U.S. (1995). Enhancing thermal conductivity of fluids with nanoparticles in Proceedings of the ASME Int. Mech. Engg Congress and Exposition, Vol. 66, pp. 995, San Francisco, USA.

Crane, L.J. (1970). Flow Past a Stretching plate, Zeitschrift frangewandte Mathematik und Physik, Vol. 21, No. 4, pp. 645–647.

Dulal, P. (2010). Mixed Convection Heat Transfer in the Boundary Layers on an Exponentially Stretching Surface with Magnetic Field, Applied Mathematics and Computation, Vol. 217, No. 6, pp. 2356–2369.

Gangaiah, T., Saidulu, N. and Lakshmi, A.V. (2018). Magnetohydrodynamic Flow of Nanofluid over an Exponentially Stretching Sheet in Presence of Viscous Dissipation and Chemical Reaction, Journal of Nanofluids, Vol. 7, No. 3, pp. 1–10.

Gupta, P.S. and Gupta, A.S. (1977). Heat and Mass Transfer on a Stretching Sheet with Suction or Blowing, The Canadian Journal of Chemical Engineering, Vol. 55, No. 6, pp. 744–746.

Hayat, T., Qasim, M. and Mesloub, S. (2011). MHD Flow and Heat Transfer over Permeable Stretching Sheet with Slip Conditions, International Journal for Numerical Methods in Fluids, Vol. 66, No. 8, pp. 963–975.

Ishak, A., Nazar, R., Bachok, N. and Pop, I. (2010). MHD Mixed Convection Flow near the Stagnation-point on a Vertical Permeable Surface, Physica A: Statistical Mechanics and its Applications, Vol. 3891, pp. 40–46.

Madhu, M. and Kishan, N. (2016). Magnetohydrodynamic Mixed Convection of a Non-Newtonian Power-law Nanofluid past a Moving Vertical Plate with Variable Density, Journal of the Nigerian Mathematical Society, Vol. 35, No. 1, pp. 199–207.

Magyari, E. and Keller, B. (1999). Heat and Mass Transfer in the Boundary Layers on an Exponentially Stretching Continuous Surface, Journal of Physics D-Applied Physics, Vol. 32, No. 5, pp. 577–585.

Malik, M.Y., Salahuddin, T., Hussain, A. and Bilal, S. (2015). MHD flow of tangent hyperbolic fluid over a stretching cylinder: Using Keller box method, Journal of Magnetism and Magnetic Materials, Vol. 395, pp. 271–276.

Masuda, H., Ebata, A., Teramae, K. and Hishinuma, N. (1993). Alteration of Thermal Conductivity and Viscosity of Liquid by Dispersing Ultra-Fine Particles, Netsu Bussei, Vol. 7, No. 4, pp. 227–233.

Mukhopadhyay, S. (2013). Slip Effects on MHD Boundary Layer Flow over an Exponentially Stretching Sheet with Suction/Blowing and Thermal Radiation, Ain Shams Engineering Journal, Vol. 4, No. 3, pp. 485–491.

Nadeem, S. and Akram, S. (2009). Peristaltic Transport of a Hyperbolic Tangent Fluid Model in an Asymmetric Channel, Zeitschrift für Naturforschung, Vol. 64(9-10), pp. 559–567.

Nield, D.A. and Kuznetsov, A.V. (2009). The Cheng-Minkowycz Problem for Natural Convective Boundary-Layer Flow in a Porous Medium Saturated by a Nanofluid, International Journal of

Heat Mass Transfer, Vol. 52, No. 2, pp. 5792–5795.

Al-Odat, M.Q., Damseh, R.A. and Al-Azab, T.A. (2006). Thermal Boundary Layer on an Exponential Stretching Continuous Surface in the presence of Magnetic Field, International Journal of Applied Mechanics and Engineering, Vol. 11, No. 2, pp. 289–299.

Pop, I. and Ingham, D.B. (2001). *Convective Heat Transfer: Mathematical and Computational Modelling of Viscous Fluids and Porous Media*, Pergamon, Oxford, Amsterdam.

Prabhakar, B., Shankar, B. and Haq, R.U. (2016). Impact of Inclined Lorentz Forces on Tangent Hyperbolic Nanofluid Flow with Zero Normal Flux of Nanoparticles at the Stretching Sheet, Neural Computing and Applications. http://dx.doi.org/10.1007/s00521-016-260-4

Reddy, C.S. and Naikoti, K. (2017). MHD Boundary Layer Flow of Casson Nanofluid Over a Non Linear Stretching Sheet with Viscous Dissipation and Convective Condition Journal of Nanofluids, Vol. 5, No. 6, pp. 870–879.

Shanker, B. and Kishan, N. (1997). The Effects of Mass Transfer on the MHD Flow past an Impulsively Started Infinite Vertical Plate with Variable Temperature or Constant Heat Flux, Journal of Energy Heat and Mass Transfer, Vol. 19, pp. 273–278.

Saidulu, N., Lakshmi, A.V. and Gangaiah, T. (2018). Thermal Radiation and Slip Effects on MHD Flow and Heat Transfer of Casson Nanofluid Over an Exponentially Stretching Sheet, Journal of Nanofluids, Vol. 7, No. 3, pp. 478–487.

Sakiadis, B.C. (1961). Boundary-layer Behaviour on Continuous Solid Surfaces: I. Boundary-layer Equations for Two-dimensional and Axisymmetric Flow, AIChE Journal, Vol. 7, No. 1, pp. 26–28.

Wang, C.Y. (1990). Liquid film on an unsteady stretching surface, Quarterly of Applied Mathematics, Vol. 48, pp. 601–610.